

# Transport properties of isospin effective mass splitting

J. Rizzo <sup>a</sup>, M. Colonna <sup>a</sup>, M. Di Toro <sup>a,1</sup> and V. Greco <sup>b</sup>

<sup>a</sup>*Laboratori Nazionali del Sud INFN, I-95123 Catania, Italy  
Physics & Astronomy Dept., Univ. of Catania*

<sup>b</sup>*Cyclotron Institute, Texas A&M University, College Station, USA*

We investigate in detail the momentum dependence ( $MD$ ) of the effective in medium Nucleon-Nucleon ( $NN$ ) interaction in the isovector channel. We focus the discussion on transport properties of the expected neutron-proton ( $n/p$ ) effective mass splitting at high isospin density. We look at observable effects from collective flows in Heavy Ion Collisions ( $HIC$ ) of charge asymmetric nuclei at intermediate energies. Using microscopic kinetic equation simulations nucleon transverse and elliptic collective flows in  $Au + Au$  collisions are evaluated. In spite of the reduced charge asymmetry of the interacting system interesting *isospin* –  $MD$  effects are revealed. Good observables, particularly sensitive to the  $n/p$ -mass splitting, appear to be the differences between neutron and proton flows. The importance of more exclusive measurements, with a selection of different bins of the transverse momenta ( $p_t$ ) of the emitted particles, is stressed. In more inclusive data a compensation can be expected from different  $p_t$ -contributions, due to the microscopic *isospin* –  $MD$  structure of the nuclear mean field in asymmetric matter.

*Key words:* Collective flows, Asymmetric nuclear matter, Nucleon effective masses, Radioactive beams

*PACS:* 21.30.Fe, 25.75.Ld, 21.65.+f, 25.60-t

## 1 Introduction

A key question in the physics of unstable nuclei is the knowledge of the *EOS* for asymmetric nuclear matter away from normal conditions. We remind again

---

<sup>1</sup> ditoro@lns.infn.it

the effect of the symmetry term at low densities on the neutron skin structure, while the knowledge in high densities region is crucial for supernovae dynamics and neutron star cooling. The paradox is that while we are planning second and third generation facilities for radioactive beams our basic knowledge of the symmetry term of the nuclear Equation of State *EOS* is still extremely poor. Effective interactions are obviously tuned to symmetry properties around normal conditions and any extrapolation can be quite dangerous. Microscopic approaches based on realistic *NN* interactions, Brueckner or variational schemes, or on effective field theories show a quite large variety of predictions, see the discussions in [1,2] and refs. therein.

In this paper we look at the mean field momentum dependence (*MD*) in the isospin channel and study its dynamical effects in heavy ion collisions at intermediate energies. This represents a completely open problem as we can quickly realize from a simple analysis of the effective Skyrme-like non-relativistic forces. Let's look at the local and non-local contributions to the potential symmetry term of various Skyrme interactions, *SIII*, *SGII*, *SKM\** (see [3] and refs. therein) and the more recent Skyrme-Lyon forms, *SLy230a* and *SLy230b* (or *Sly4*), [4]. We can clearly see a sharp transition from the previous Skyrme forces to the Lyon parametrizations, with an almost inversion of the signs of the two contributions. The important repulsive non-local part of the Lyon forces leads to a completely different behavior of the neutron matter *EOS*, of great relevance for the neutron star properties. Actually this substantially modified parametrization was mainly motivated by a very unpleasant feature in the spin channel of the previous Skyrme forces, the collapse of polarized neutron matter, see discussion in [5,4].

A related interesting effect can be seen on the neutron/proton effective masses. For an asymmetry  $\beta \equiv \frac{N-Z}{A} = 0.2$  (the  $^{197}\text{Au}$  asymmetry) we can get a splitting up to the order of 15% at normal density  $\rho_0$ , and increasing with baryon density.

The sign itself of the splitting is very instructive. Passing from Skyrme to Skyrme-Lyon we see a dramatic inversion in the sign of the *n/p* mass splitting. The Lyon forces predict in *n*-rich systems a neutron effective mass always smaller than the proton one. We will come back to this point. Here we just note that the same result is obtained from more microscopic relativistic Dirac-Brueckner calculations [6] and in general from the introduction of scalar isovector virtual mesons in Relativistic Mean Field (*RMF*) approaches [7,8]. At variance, non-relativistic Brueckner-Hartree-Fock calculations are leading to opposite conclusions [9,10]. This will be one of the main questions to address in the reaction dynamics of exotic nuclear systems.

We can expect important effects on transport properties ( fast particle emission, collective flows, resonance and particle production around the threshold)

of the dense and asymmetric  $NM$  that will be reached in Radioactive Beam collisions at intermediate energies.

This is the aim of the present paper. We focus our attention on the isospin dependence of collective flows. We perform collision simulations based on microscopic kinetic equation models. We start from realistic effective interactions widely used for symmetric systems. We test very different parametrizations in the momentum dependence of the isovector channel, taking care that the symmetry energy, including its density dependence, will be not modified. We study in particular the transport effect of the sign of the  $n/p$  effective mass splitting  $m_n^* - m_p^*$  in asymmetric matter at high baryon and isospin density.

We see very interesting *isospin* – *MD* effects on  $n/p$  transverse and elliptic flows in semicentral  $Au + Au$  collisions at 250  $AMeV$  beam energy. The importance of more exclusive data, with a good selection of the transverse momenta of the emitted particles, is stressed.

In Sect.2 we present details of the chosen effective interactions. In Sect.3 the collective flow results are discussed and finally in Sect.4 some conclusions are drawn with relative perspectives.

## 2 The choice of the effective interactions

The phenomenological non-relativistic effective *EOS* used in this work was first introduced by I.Bombaci et al. [11,12] in a general form suitable for astrophysical and heavy ion physics applications. We have modified the isovector part in order to get two new parametrizations with different  $n/p$  effective mass splittings while keeping the same symmetry energy at saturation, including a very similar overall density dependence.

We start writing down the energy density as a function of the asymmetry parameter  $\beta \equiv \frac{N-Z}{A}$ :

$$\varepsilon(\rho_n, \rho_p) = \varepsilon_{kin} + \varepsilon_A + \varepsilon_B + \varepsilon_{MD} \quad (1)$$

$$\varepsilon_{kin}(\rho_n, \rho_p) = \frac{2}{(2\pi)^3} \int d^3k f_n(k) \frac{\hbar^2}{2m} k^2 + \frac{2}{(2\pi)^3} \int d^3k f_p(k) \frac{\hbar^2}{2m} k^2$$

$$\varepsilon_A(\rho, \beta) = \frac{A}{2} \frac{\rho^2}{\rho_0} - \frac{A}{3} \frac{\rho^2}{\rho_0} \left( \frac{1}{2} + x_0 \right) \beta^2$$

$$\varepsilon_B(\rho, \beta) = \frac{B}{\sigma + 1} \frac{\rho^{\sigma+1}}{\rho_0^\sigma} - \frac{2}{3} \frac{B}{\sigma + 1} \frac{\rho^{\sigma+1}}{\rho_0^\sigma} \left( \frac{1}{2} + x_3 \right) \beta^2$$

$$\varepsilon_{MD}(\rho_n, \rho_p, \beta) = C \frac{\rho}{\rho_0} (\mathcal{I}_n + \mathcal{I}_p) + \frac{C - 8z_1}{5} \frac{\rho}{\rho_0} \beta (\mathcal{I}_n - \mathcal{I}_p)$$

where the integrals  $\mathcal{I}_\tau(k, \Lambda) = \frac{2}{(2\pi)^3} \int d^3k f_\tau(k) g(k, \Lambda)$  include the momentum dependent part of the mean field  $g(k, \Lambda) = \left[ 1 + \left( \frac{k - \langle k \rangle}{\Lambda} \right)^2 \right]^{-1}$ ; the subscript  $\tau = n, p$  stands for neutrons and protons respectively;  $\rho_0 = 0.16 \text{ fm}^{-3}$  is the normal density of nuclear matter. We refer to this parametrization as the *BGBD – EOS*. For symmetric nuclear matter ( $\beta = 0$ ), the energy density Eq.(1) reduces to the parametrization proposed by Gale, Bertsch and Das Gupta (*GBD* interaction, [13]). The parameters  $A, B, C, \sigma$  and  $\Lambda$  take the same values as in [13] ( $A = -144 \text{ MeV}, B = 203.3 \text{ MeV}, C = -75 \text{ MeV}, \sigma = \frac{7}{6}, \Lambda = 1.5 p_F^{(0)}$ , where  $p_F^{(0)}$  is the Fermi momentum at normal density), and provide a soft EOS for symmetric matter, with a compressibility  $K_{NM} \simeq 210 \text{ MeV}$ .

The value of  $z_1$  sets the strength of the momentum dependence (*MD*) in the isospin channel; the remaining parameters  $x_0$  and  $x_3$  can be set to fix the symmetry energy.

Taking the functional derivative of the energy density with respect to the distribution function  $f_\tau$ , we obtain, apart from the kinetic term  $\varepsilon_{kin}$ , the mean field potential for neutrons and protons:

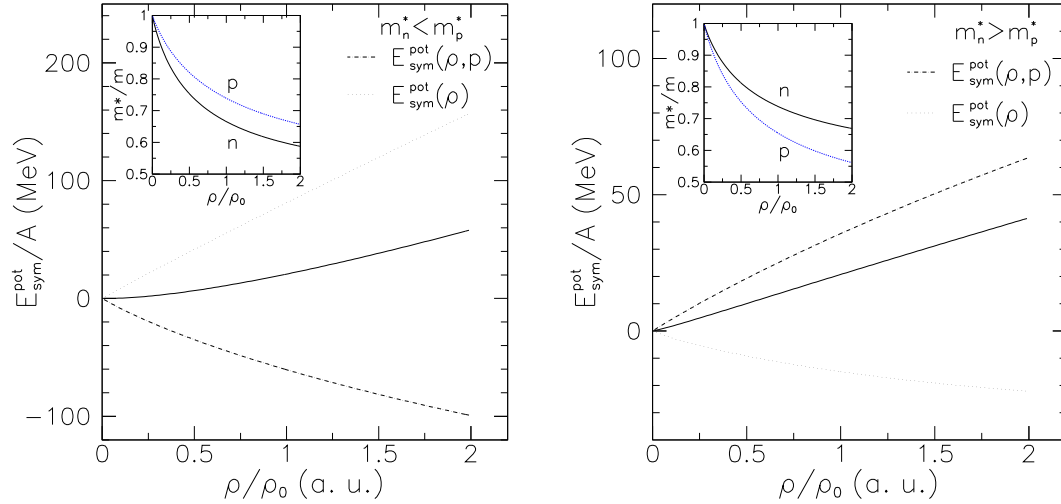


Fig. 1. Potential symmetry energy as a function of density (solid line) for  $m_n^* < m_p^*$  (left) and  $m_n^* > m_p^*$  (right). Dotted lines refer to density-dependent contributions, dashed-dotted to momentum dependent ones. Small panels indicate the corresponding behaviour of proton and neutron effective masses as a function of density, with  $\beta = 0.2$ .

$$\begin{aligned}
U_\tau(k; \rho, \beta) = & A \left( \frac{\rho}{\rho_0} \right) + B \left( \frac{\rho}{\rho_0} \right)^\sigma - \frac{2}{3}(\sigma - 1) \frac{B}{\sigma + 1} \left( \frac{1}{2} + x_3 \right) \left( \frac{\rho}{\rho_0} \right)^\sigma \beta^2 \\
& \pm \left[ -\frac{2}{3} A \left( \frac{1}{2} + x_0 \right) \left( \frac{\rho}{\rho_0} \right) - \frac{4}{3} \frac{B}{\sigma + 1} \left( \frac{1}{2} + x_3 \right) \left( \frac{\rho}{\rho_0} \right)^\sigma \right] \beta \quad (2) \\
& + \frac{4}{5\rho_0} \left\{ \frac{1}{2} (3C - 4z_1) \mathcal{I}_\tau + (C + 2z_1) \mathcal{I}_{\tau'} \right\} \\
& + \left( C \pm \frac{C - 8z_1}{5} \beta \right) \left( \frac{\rho}{\rho_0} \right) g(k)
\end{aligned}$$

where the subscripts in the integrals are  $\tau \neq \tau'$ ; the upper signs refer to neutrons, the lower ones to protons. Protons and neutrons in asymmetric matter experience different interactions; when  $\beta = 0$  we return to the *GBD* mean field. It is known that a mean field *MD* implies the idea of an in-medium reduction of nucleon mass and leads to the introduction of effective mass [14].

The last *BGBD* term includes, besides the usual *GBD* momentum dependence, an isospin-dependent part from which we get different effective masses for protons and neutrons. In fact, the effective mass has the following definition:

$$\frac{m_\tau^*}{m} = \left\{ 1 + \frac{m}{\hbar^2 k} \frac{dU_\tau}{dk} \right\}_{k=k_F^{[\tau]}}^{-1} \quad (3)$$

and we see that mass splitting is determined not only by different momentum

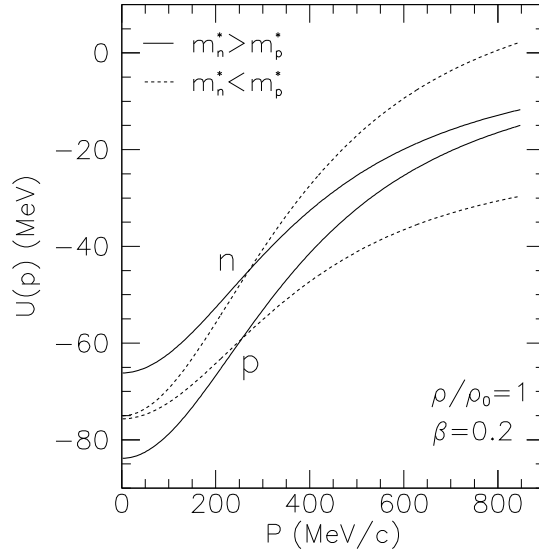


Fig. 2. Mean field potential as a function of momentum at normal density, for an asymmetry  $\beta = 0.2$ . Solid lines refer to the case  $m_n^* > m_p^*$ , dashed lines to  $m_n^* < m_p^*$ .

dependence of mean field, but also by Fermi momenta of neutrons and protons. In our case we get:

$$\frac{m_\tau^*}{m} = \left\{ 1 + \frac{-\frac{2m}{\hbar^2} \frac{1}{\Lambda^2} \left( C \pm \frac{C-8z_1}{5} \beta \right) \frac{\rho}{\rho_0}}{\left[ 1 + \left( \frac{k_{F0}}{\Lambda} \right)^2 (1 \pm \beta)^{(2/3)} \left( \frac{\rho}{\rho_0} \right)^{(2/3)} \right]^2} \right\}^{-1}$$

In order to investigate the effects of mass splitting on non-relativistic heavy ion collisions we choose two sets of parameters (shown in Table 1) which give opposite splitting, but quite similar behaviour of the symmetry energy.

mass splitting	$z_1$	$x_0$	$x_3$
$m_n^* > m_p^*$	-36.75	-1.477	-1.01
$m_n^* < m_p^*$	50	1.589	-0.195

Table 1

Values of the parameters  $z_1$ ,  $x_0$  and  $x_3$  for opposite mass splitting, giving the same  $E_{sym}(\rho_0) = 33 \text{ A MeV}$ .

Assuming the usual parabolic law for the EOS of asymmetric nuclear matter:

$$\frac{E}{A}(\rho, \beta) = \frac{E}{A}(\rho) + \frac{E_{sym}}{A}(\rho)\beta^2$$

we fix the same symmetry energy at the saturation density  $E_{sym}(\rho_0) = 33 \text{ A MeV}$ .

Figure 1 shows the potential part of the symmetry energy as a function of density (solid line) for the two choices of mass splitting. We remark the very similar overall density dependence. The dashed-dotted and dotted lines indicate respectively the contributions from the momentum dependent and density-dependent part of the EOS. A change in the relative sign of mass splitting is related to opposite behaviours of these two contributions, exactly as already noticed in the Introduction for the Skyrme-like forces. Small panels on the top left of each graph illustrate the corresponding mass splitting as a function of density for an asymmetry  $\beta = 0.2$  (the  $^{197}\text{Au}$  asymmetry).

Let us discuss now the relation between effective mass and momentum dependence. From the definition Eq.(3) we see that the effective mass is inversely proportional to the slope of mean field at the Fermi momentum. Then, for nucleons with smaller effective masses the potential will be more repulsive at momenta higher than the Fermi one, and more attractive at low momenta. Mean field potential at normal density as a function of momentum is shown in Figure 2 for a choice  $\beta = 0.2$ . As we see, the parametrizations used in this work give rise to opposite behaviors for low and high momentum particles. This is a very general feature, due to the meaning itself Eq.(3) of effective mass. As we will see in the reaction dynamics this behavior can give rise to

some compensation effects between low and high momenta contributions. All that will lead to an expected larger *isospin* – *MD* sensitivity of more exclusive measurements, in particular with a transverse momentum selection of the nucleons emitted for a given rapidity.

### 3 Effective Masses and Collective Flows

Collective flows in heavy ion reactions have been widely used to investigate properties of nuclear matter, such as compressibility or in-medium cross sections [15], isospin dependence [16,17,18] and to find out signals of the mean field *MD* ([19], [20]). The problem of momentum dependence in the isospin channel is still open, and recently some possible effects at relativistic energies have been studied [21]. Intermediate energies are important in order to have high momentum particles and to test regions of high baryon (isoscalar) and isospin (isovector) density during the reactions dynamics. Now we present some qualitative features of the dynamics in heavy ion collisions related to the splitting of nucleon effective masses.

Our simulations are performed by means of the Boltzmann-Nordheim-Vlasov *BNV* transport code from Ref. [22], implemented with a *BGBD-like* mean field, and using free (isospin dependent) isotropic cross sections in the collision term. We focus on semi-peripheral *Au + Au* collisions at the energy of 250 *AMeV* and we evaluate transverse and elliptic flows of neutrons and pro-

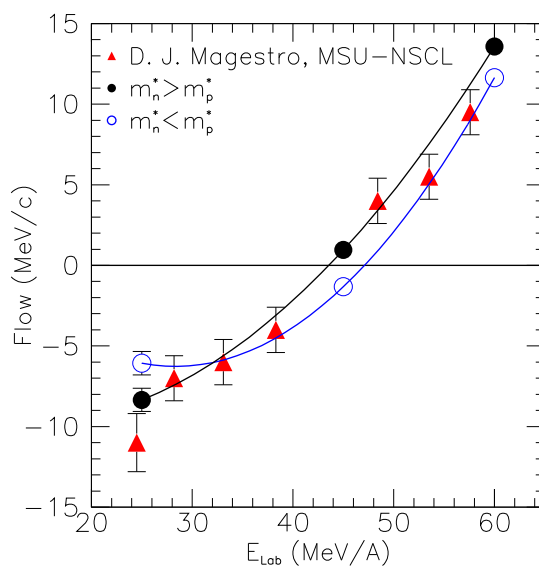


Fig. 3. Balance energy in *Au + Au* collisions for intermediate impact parameters. Solid circles refer to the case  $m_n^* > m_p^*$ , empty circles to  $m_n^* < m_p^*$ . Triangles represent the data from ref.[25]

tons. We consider as emitted particles those resulting in density regions below  $1/8 \rho_0$  during the reaction. We have checked that the results are not depending on the size of the box where the simulation is performed and on the choice of the freeze-out time.

These flow observables can be seen respectively as the first and second coefficients from the Fourier expansion of the azimuthal distribution:

$$\frac{dN}{d\phi}(y, p_t) = 1 + V_1 \cos(\phi) + 2V_2 \cos(2\phi)$$

where  $p_t = \sqrt{p_x^2 + p_y^2}$  is the transverse momentum and  $y$  the rapidity along beam direction.

### 3.1 Transverse flows

The transverse flow can be expressed as:

$$V_1(y, p_t) = \left\langle \frac{p_x}{p_t} \right\rangle$$

It provides information on the azimuthal anisotropy of the transverse nucleon emission and has been recently used to study the *EOS* and cross section sensitivity of the balance energy [15].

Actually the evaluation of the balance energy for the proton more inclusive *Directed Flow*, integrated over all transverse momenta see [23,16], in  $Au + Au$  collisions represents a very good test for our effective interactions at lower energies. The results are shown in Fig.3 and compared with NSCL-MSU data. Our proton directed flows are calculated for semicentral collisions, i.e.  $b_{red} = 0.5$  [24].

Both parametrizations are well reproducing the experimental balance energy region. As expected we see a slightly earlier balance of the flow in the  $m_n^* > m_p^*$  case due to some more repulsion for fast protons but the effect is hardly appreciable at these energies. We will look more carefully at these effects with increasing beam energy and for more exclusive observables.

We will present now  $n/p$  transverse flow results for semicentral  $^{197}Au + ^{197}Au$  collisions at 250 *AMeV* beam energy, for particles in regions of relatively high rapidities. It is useful to work with momenta and rapidities normalized to projectile ones in the center of mass system (*cm*), defined as  $y^{(0)} \equiv (y/y_{proj})_{cm}$  and  $p_t^{(0)} \equiv (p_t/p_{proj})_{cm}$ . Results of our calculations are illustrated in Fig. 4, where the left and right panels illustrate the two cases  $m_n^* < m_p^*$  and  $m_n^* > m_p^*$  respectively.



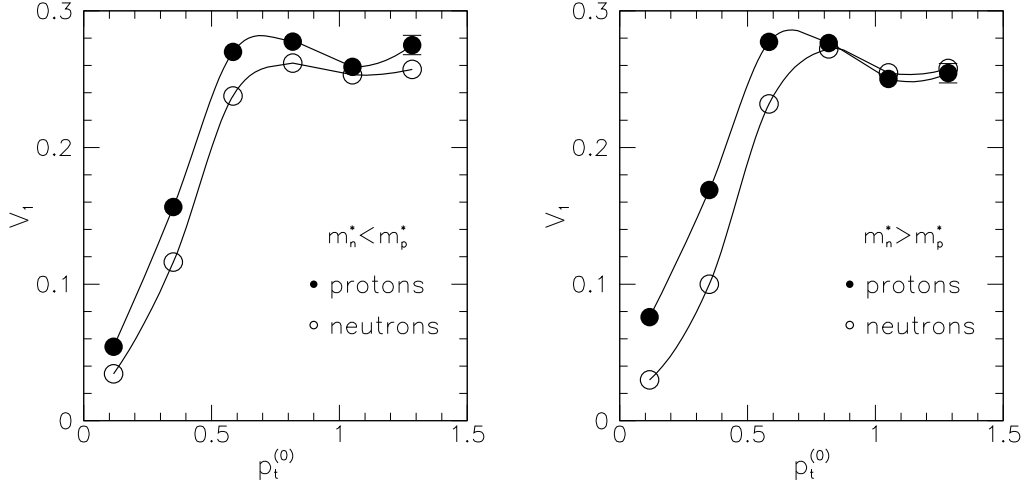


Fig. 4. Transverse flow of protons and neutrons for Au+Au reactions at 250 A MeV,  $b/b_{max} = 0.5$ , in the rapidity interval  $0.7 \leq |y^{(0)}| \leq 0.9$ .

High rapidity selections allow us to find effects of the mean field  $MD$ , which becomes more important with increasing momenta. Indeed the different behaviour of mean field depending on mass splitting is evident all over the range of transverse momentum shown here. We emphasize that the average momentum of these particles is generally beyond the Fermi momentum. Indeed a rough estimate in the center of mass system gives already for the beam parallel

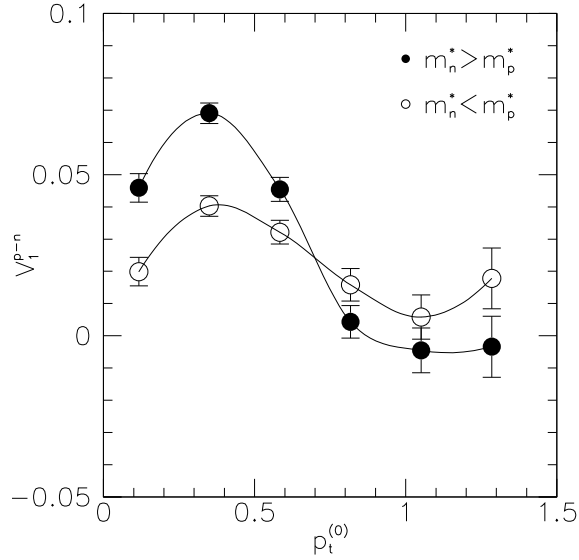


Fig. 5.  $p_t$  dependence of the difference between neutron and proton transverse flows in Au + Au collisions, same energy, centrality and rapidity selection as in Fig.4. Solid circles refer to the case  $m_n^* > m_p^*$ , empty circles to  $m_n^* < m_p^*$ .

component

$$p_z \approx m_0 \cdot 0.8(y_{proj})_{cm} \simeq 260 - 280 \text{ MeV}/c$$

In this momentum region a smaller effective mass determines greater repulsive interaction. When  $m_n^* < m_p^*$  neutrons feel greater repulsion than protons and their deflection in the reaction plane for  $p_t^{(0)} \leq 0.6$  is close to protons, where the Coulomb field is also acting. At variance in the case  $m_n^* > m_p^*$  the proton flow is greatly enhanced if compared with neutrons.

At high transverse momentum we must take into account the increase of the out-of-plane component, so in this case increased repulsion determines a greater reduction of transverse flow. It causes a crossing between proton and neutron flow in the case  $m_n^* > m_p^*$ . This behaviour is clearly seen if we look at the different slope of the curves in Fig. 4 (right panel) around  $p_t^{(0)} \geq 0.6$ .

A quite suitable way to observe such effective mass splitting effect on the transverse flows is to look directly at the difference between neutron and proton flows

$$V_1^{p-n}(y, p_t) \equiv V_1^p(y, p_t) - V_1^n(y, p_t)$$

shown in Fig.5.

Now the variation due to the mass splitting choice is quite evident in the whole  $p_t$  range of emitted nucleons. Since the statistics is much smaller at high  $p_t$ 's (large error bars in the evaluation) the effect should be mostly observed in the  $p_t^{(0)} \leq 0.5$  range.

### 3.2 Elliptic flows

The competition between in-plane and out-of-plane emissions can be pointed out by looking at the elliptic flow, which has the following expression:

$$V_2(y, p_t) = \langle \frac{p_x^2 - p_y^2}{p_t^2} \rangle$$

The sign of  $V_2$  indicates the azimuthal anisotropy of emission: particles can be preferentially emitted either in the reaction plane ( $V_2 > 0$ ) or out-of-plane (squeeze-out,  $V_2 < 0$ ).

Also in this case a good check of our effective interaction choices is provided by some more inclusive data in the medium energy range. In Fig.6 we report a comparison with the *FOPi* – *GSI* data in the interesting beam energy region of the change of sign of the elliptic flow for protons, integrated over large transverse momentum contributions. The agreement is reasonable for both parametrizations. Also in this case we see a slightly larger overall repulsion (earlier zero-crossing) for the  $m_n^* > m_p^*$  case.

Our results on the  $p_t$  dependence of the neutron/proton elliptic flows in  $Au + Au$  reactions at 250  $AMeV$  are shown in Fig. 7. We can see that the  $p_y$  component rapidly grows at momenta  $p_t^{(0)} > 0.6$ , causing the flows to fall down towards negative values. At low momenta, emitted particles undergo a deflection in the reaction plane, more pronounced for nucleons with smaller effective mass. In fact, comparing the two panels of Fig.7 we see that around the maximum in-plane deflection  $0.4 \lesssim p_t^{(0)} \lesssim 0.8$  neutron and proton flows are inverted. We also find different slopes for protons and neutrons around  $p_t^{(0)} \geq 0.7$ , depending on the relative sign of mass splitting, in agreement with the previous results in the transverse flows. Around  $p_t^{(0)} \simeq 1$ , i.e. projectile momentum in the  $cm$ , the elliptic flow finally takes negative values, with slight differences for the two parametrizations.

Also in this case the best observable to look at is the  $p_t$  dependence of the difference between neutron and proton elliptic flows

$$V_2^{p-n}(y, p_t) \equiv V_2^p(y, p_t) - V_2^n(y, p_t)$$

shown in the Fig.8.

Again the difference is quite evident in the whole  $p_t$  range of emitted nucleons. We note again that the statistics is much smaller at high  $p_t$ 's (large error bars in the evaluation). Anyway the mass splitting effect appears very clearly in the low  $p_t^{(0)} \leq 0.5$  range where the results are more reliable.

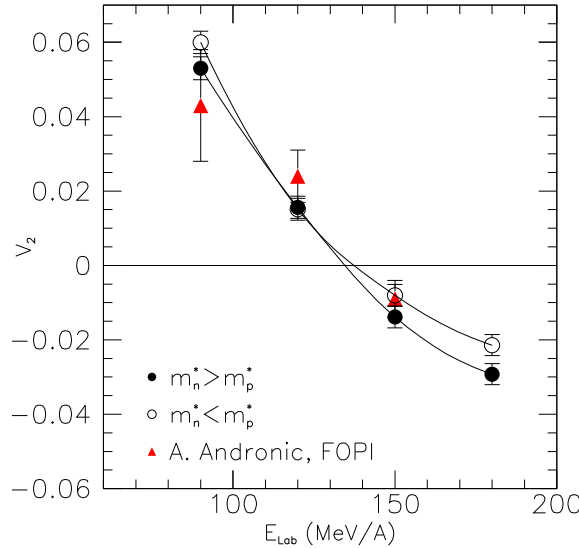


Fig. 6. Energy dependence of the elliptic flow in  $Au + Au$  semicentral collisions at mid-rapidity,  $|y^{(0)}| \leq 0.1$ , integrated over the  $p_t^{(0)} \geq 0.8$  range. *FOPI* data with similar selections, see ref. [26], are given by the full triangles. Solid circles refer to the case  $m_n^* > m_p^*$ , empty circles to  $m_n^* < m_p^*$ .

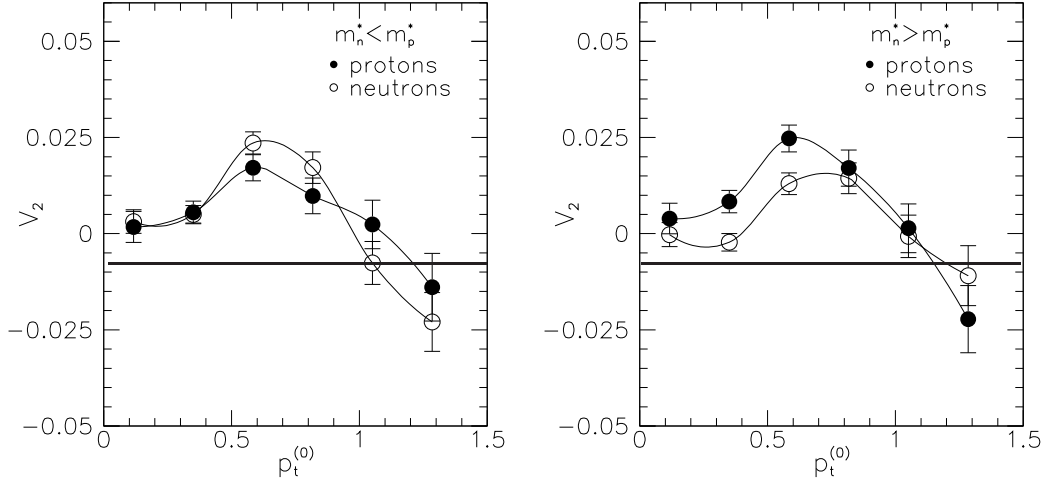


Fig. 7. Elliptic flow of protons and neutrons in Au+Au reaction at 250 A MeV,  $b/b_{max} = 0.5$ , in the rapidity interval  $0.7 \leq |y^{(0)}| \leq 0.9$ .

As a general comment we stress the importance of more exclusive data, with a good  $p_t$  selection. Indeed from Figs. 4, 5 (for  $V_1$ ) and Figs. 7, 8 (for  $V_2$ ) we clearly see that more inclusive  $V_1(y)$ ,  $V_2(y)$  data, integrated over all  $p_t$ 's of the emitted nucleons at a given rapidity, will appear to be less sensitive to *isospin* – *MD* effects. As already discussed from general features of the mean field *MD* we expect a kind of compensation between low and high  $p_t$  contributions.

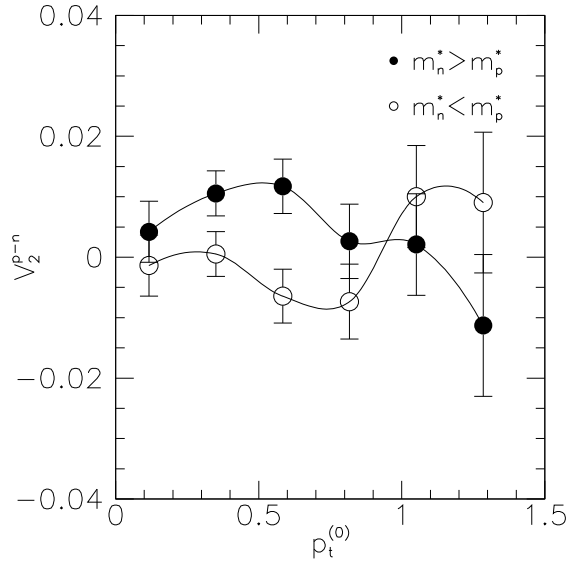


Fig. 8.  $p_t$  dependence of the difference between neutron and proton transverse flows in Au + Au collisions, same energy, centrality and rapidity selection as in Fig.7. Solid circles refer to the case  $m_n^* > m_p^*$ , empty circles to  $m_n^* < m_p^*$ .

### 3.3 Low rapidity results

In order to confirm the interpretation of the previous flow results we have performed the same analysis for a low rapidity selection  $0 \leq |y^{(0)}| \leq 0.25$ . Since we are now looking at particles with overall smaller momenta, the effects of the isospin contributions to the mean-field- $MD$  should be reduced.

We illustrate this point in Fig.9, where the difference between proton and neutron flows are plotted as a function of transverse momentum in the low rapidity region. We have behaviors quite similar to the corresponding Figs.5, 8, but the effective mass splitting cannot be clearly observed.

We can see some indications of a larger attraction felt by low momenta protons in the case  $m_n^* > m_p^*$ , see the  $p$ -solid line of Fig.2. This can be observed in the reduction of the proton transverse flow at low  $p_t^{(0)}$ , solid circles below the empty ones in the range  $p_t^{(0)} \leq 0.5$ . The effect looks interesting, although not much appreciable because of large uncertainty.

### 3.4 Changing the stiffness of the symmetry term

It is well known that the collective flows for asymmetric systems are sensitive to the density dependence of the symmetry term of the nuclear EOS, in particular at high transverse momentum [16,17,18].

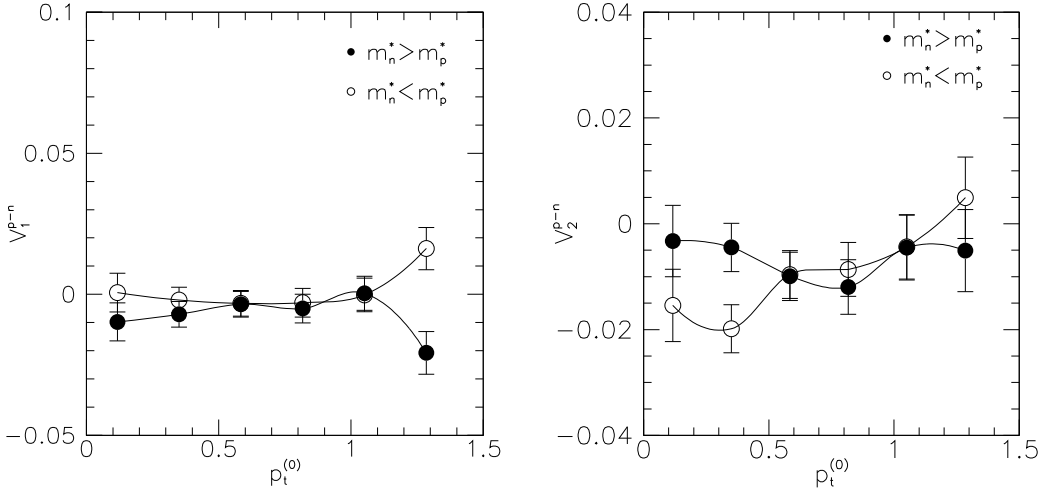


Fig. 9.  $p_t$  dependence of the difference between neutron and proton transverse (left panel) and elliptic flow (right panel) in  $Au + Au$  collisions at 250 A MeV,  $b/b_{max} = 0.5$ , in the rapidity interval  $0 \leq |y^{(0)}| \leq 0.25$ . Solid circles refer to the case  $m_n^* > m_p^*$ , empty circles to  $m_n^* < m_p^*$ .

mass splitting	$z_1$	$x_0$	$x_3$
$m_n^* > m_p^*$	-36.75	0.11	0.21
$m_n^* < m_p^*$	50	4.449	2.

Table 2

Values of the parameters  $z_1$ ,  $x_0$  and  $x_3$  for opposite mass splitting, giving a similar soft symmetry term.

For this reason it is important to be sure that signals previously discussed are mainly due to the  $n/p$  effective mass splitting and not strictly depending on the choice of the stiffness of the symmetry energy.

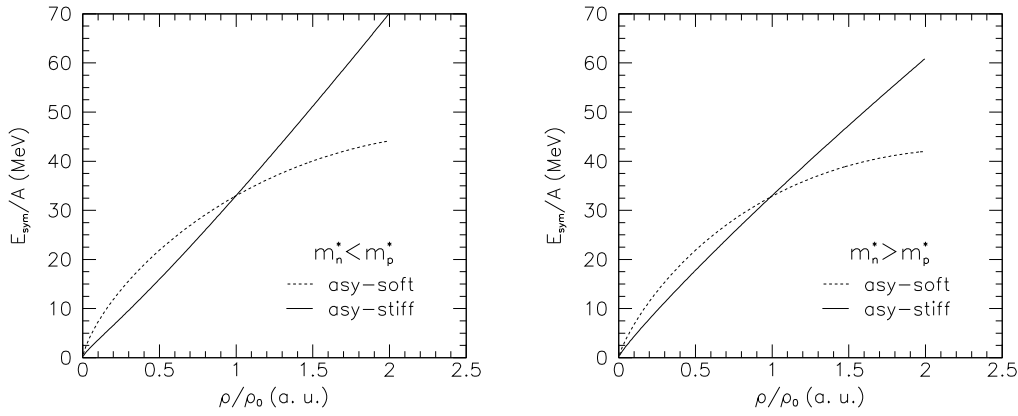


Fig. 10. Total symmetry energy as a function of density for the two mass splitting choices used in this work. Solid and dashed lines represent respectively the *asy-stiff* and *asy-soft* equations of state.

In order to check this point we have performed some calculations using a symmetry energy with a density behaviour very different from the one used before, *but keeping the same  $n/p$ -effective mass splittings*. We refer to it as *asy-soft*, see Fig.10, compared with the *asy-stiff* previously used (shown also in Fig.1 for the potential part). Since aim is to leave the momentum dependence of the symmetry potential unchanged and to modify only the density dependence, we take the same  $z_1$  values used before and choose new  $x_0$  and  $x_3$  values. In this way we can generate a softer symmetry energy at high density, of course with the same saturation value  $E_{sym}(\rho_0) = 33 \text{ A MeV}$ . Table 2 reports the two sets of new parameters.

In Fig. 10 we show the total (potential plus kinetic) symmetry energy in the two cases,  $m_n^* < m_p^*$  (left panel) and  $m_n^* > m_p^*$  (right panel). Solid and dashed lines represent respectively the *asy-stiff* and *asy-soft* curves.

Our results show that while the nucleon flows are depending on the stiffness

of the symmetry term, like in other calculations [16,17,18], the transverse momentum behavior of the differences keeps the same sensitivity to the effective mass splittings.

Fig. 11 illustrates the  $n/p$ -flow differences as a function of transverse momentum for the same energy, impact parameter and high rapidity selections used before. Both transverse  $V_1^{p-n}(y, p_t)$  and elliptic  $V_2^{p-n}(y, p_t)$  flow differences show very small variations from the *asy - stiff* case (i.e. Figs. 5 and 8) over the whole  $p_t^{(0)}$  range, in particular in the region  $p_t^{(0)} \leq 0.5$ , of interest for the better statistics.

This result represents an important indication that we are selecting experimental observables that directly probe the isospin effects on the momentum dependent part of the nuclear *EOS*.

#### 4 Conclusion and outlook

We have presented some expected influence of the momentum dependence in the isovector channel of the effective  $NN$  interaction on the heavy ion reaction dynamics at intermediate energies.

For a given parametrization, dynamical effects of momentum dependence in the isospin channel are opposite for neutrons and protons, so that they can be

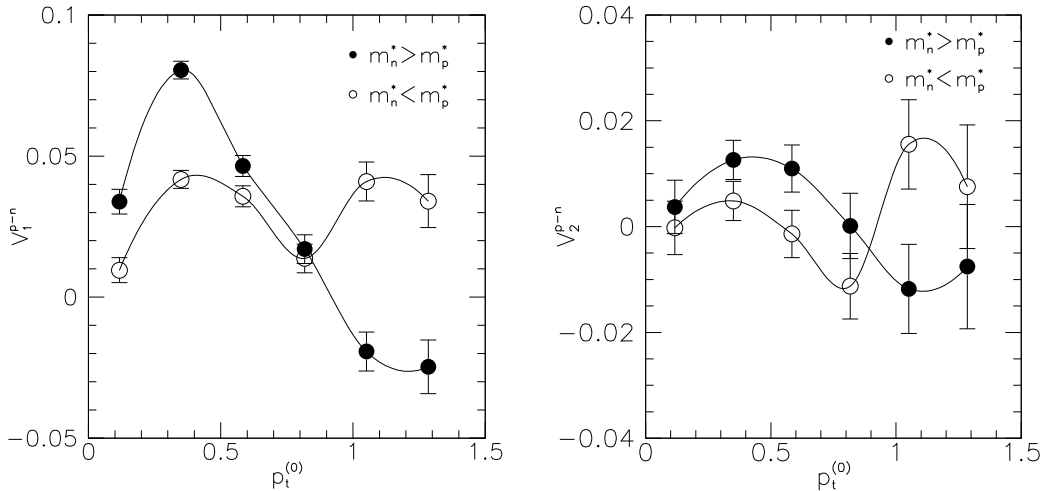


Fig. 11.  $p_t$  dependence of the difference between neutron and proton transverse (left panel) and elliptic flow (right panel) in  $Au + Au$  collisions at  $250 A\text{MeV}$ ,  $b/b_{max} = 0.5$ , in the rapidity interval  $0.7 \leq |y^{(0)}| \leq 0.9$ . Calculations are performed using the *asy - soft* symmetry energy. Solid circles refer to the case  $m_n^* > m_p^*$ , empty circles to  $m_n^* < m_p^*$ .

magnified by looking at the differences between neutron and proton collective flows. This kind of measurements requires the detection of neutron flows, but it is very useful to draw out some information about the relative sign of the effective mass splitting in a asymmetric nuclear medium.

In spite of the low asymmetry we have found interesting effects from the study of  $Au+Au$  semicentral collisions at 250  $AMeV$ . These results can provide some hints for future measurements, also with unstable beams.

We suggest to look at the flows of particles of relatively large rapidity, in particular performing more exclusive experiments for various transverse momentum selections. A compensation is indeed expected for observables where all  $p_t$  contributions are summed up. This is physically understandable on general grounds due to the different interplay between low and high momentum mean field repulsion, for the various effective mass choices.

These more exclusive flow observables, in particular the transverse  $V_1^{p-n}(y, p_t)$  and elliptic  $V_2^{p-n}(y, p_t)$  flow differences, appear to be very selective probes of the momentum dependence of the isovector part of the nuclear  $EOS$ . The observed effects are not changing when we largely modify the density dependence of the symmetry term while keeping unchanged the momentum dependence of the symmetry mean field.

Due to the difficulty of the neutron flow detection, good data with similar features could be obtained from the flows of light isobars, like  $^3H, ^3He$  and so on. Exclusive data, with a  $p_t$  selection, appear in any case of large importance.

Collective flow measurements seem to represent a very nice exploration of the highly controversial sign of the  $n/p$  effective mass splitting in asymmetric matter, of large fundamental interest. Moreover related important effects can be expected in a wide spectrum of the nuclear physics phenomenology, from the structure of drip-line nuclei to the threshold production of resonances and particles in  $HIC$  with radioactive beams.



## References

- [1] *Isospin Physics in Heavy-ion Collisions at Intermediate Energies*, Eds. Bao-An Li and W. Udo Schroeder, Nova Science Publishers (2001, New York)
- [2] M.Di Toro et al.: Nucl. Phys. **A722**, 129c (2003).
- [3] H.Krivine, J.Treiner and O.Bohigas: Nucl. Phys. **A336**, 155 (1980).
- [4] E.Chabanat, P.Bonche, P.Haensel, J.Meyer, R.Schaeffer: Nucl. Phys. **A627**, 710 (1997).
- [5] M.Kutschera and W.Wojcik: Phys. Lett. **B325**, 271 (1994).
- [6] F.Hofmann, C.M.Keil, H.Lenske: Phys. Rev. **C64**, 034314 (2001)
- [7] B.Liu, V.Greco, V.Baran, M.Colonna and M.Di Toro: Phys. Rev. **C65**, 045203 (2002)
- [8] V.Greco, M.Colonna, M.Di Toro, F.Matera: Phys. Rev. **C67**, 015203 (2003)
- [9] W.Zuo, I.Bombaci and U.Lombardo: Phys. Rev. **C60**, 24605 (1999).
- [10] W.Zuo, A.Lejeune, U.Lombardo and J.F.Mathiot: Eur. Phys. J. **A14**, 469 (2002).
- [11] I. Bombaci et al.: Nucl. Phys. **A583**, 623 (1995).
- [12] I.Bombaci, "EOS for isospin-asymmetric nuclear matter for astrophysical applications", in [1] pp. 35-81.
- [13] C. Gale, G.F.Bertsch and S.Das Gupta: Phys. Rev. **C41**, 1545 (1990).
- [14] G.F. Bertsch and S. Das Gupta: Phys. Rep. **160**, 189 (1988).
- [15] B.A. Li and A.T. Sustich: Phys. Rev. Lett. **82**, 5004 (1999).
- [16] L.Scalone, M.Colonna and M.Di Toro: Phys. Lett. **B461**, 9 (1999).
- [17] B.A. Li: Phys. Rev. Lett **85**, 4221 (2000).
- [18] B.A. Li, A.T. Sustich and B. Zhang: Phys. Rev. **C64**, 054604 (2001).
- [19] J. Zhang et al.: Phys. Rev. **C50**, 1617 (1994).
- [20] P. Danielewicz: Nucl. Phys. **A673**, 375 (2000).
- [21] V. Greco et al.: Phys. Lett. **B562**, 215 (2003).
- [22] V. Greco, Diploma Thesis (1997);  
V.Greco, A.Guarnera, M.Colonna and M.Di Toro: Phys. Rev. **C59**, 810 (1999).
- [23] G.Westfall: Nucl. Phys. **A630**, 27c (1998) and refs. therein.
- [24] The reduced impact parameter is defined as  $b_{red} \equiv b/b_{max}$  where  $b_{max}$  is the sum of the two nuclear radii.

- [25] D.J.Magestro et al.: Phys. Rev. **C61**, 021602 (2000).
- [26] A.Andronic et al.: Nucl. Phys. **A661**, 333c (1999).